



Article

Detecting differential transcription factor activity from ATAC-seq data

Ignacio J. Tripodi^{1,2} , Mary A. Allen² , Robin D. Dowell^{1,2,3,*} 

¹ Computer Science, University of Colorado, Boulder;

² BioFrontiers Institute, University of Colorado, Boulder;

³ Molecular, Cellular and Developmental Biology, University of Colorado, Boulder

* Correspondence: robin.dowell@colorado.edu; Tel.: +1-303-492-8204

Version May 6, 2018 submitted to *Molecules*

Abstract: Transcription factors are managers of the cellular factory, and key components to many diseases. Many non-coding single nucleotide polymorphisms affect transcription factors, either by directly altering the protein or its functional activity at individual binding sites. Here we first briefly summarize high throughput approaches to studying transcription factor activity. We then demonstrate, using published chromatin accessibility data (specifically ATAC-seq), that the genome wide profile of TF recognition motifs relative to regions of open chromatin can determine the key transcription factor altered by a perturbation. Our method of determining which TF are altered by a perturbation is simple, quick to implement and can be used when biological samples are limited. In the future, we envision this method could be applied to determining which TFs show altered activity in response to a wide variety of drugs and diseases.

Keywords: transcription factor; perturbation; RNA-seq; DNase I cleavage; ATAC-seq; open chromatin; motif; DASTk

1. Introduction

Transcription factors (TFs) are the managers of the cellular factory, controlling everything from cellular identity to response to external stimuli[1]. Because of their central importance in interpreting the genome, millions of people are affected by mutations residing within TFs[2], causing a wide variety of symptoms (see Table 1). For example, over half of all cancers have a mutation in the TF TP53[3].

Table 1. Examples of diseases caused by mutations in a transcription factor.

Mutated TF	Disease/Symptoms
RUNX1	Familial platelet disorder with associated myeloid malignancy[4]
GRHL3	Cleft Palate[5]
MITF	Deafness[6]; Waardenburg syndrome (hearing loss)[7]
LMX1B	Nail-patella syndrome[8] (poorly developed nails and kneecaps)
TFAM	Mitochondrial DNA depletion syndrome[9]
NKX2-5	Congenital heart disease[10]
TBX5	Holt-Oram syndrome[11] (impaired development of the heart and upper limbs)
MAF	Congenital cataract[12] (severe visual impairment in infants)
TCF4	Pitt-Hopkins syndrome[13] (intellectual disability and developmental delay, breathing problems, recurrent seizures)

Moreover, most disease-causing mutations are found in regulatory regions[14,15], e.g. enhancers, which are dense with TF binding sites[16]. A startling 60-76.5% of disease-associated single nucleotide

20 polymorphisms (SNPs) are in enhancers[17–20], which are short regulatory regions densely bound by
21 TFs[21]. In fact, the well known program HaploReg now lists all TFs that bind over each SNP, a useful
22 piece of information for understanding the impact of a SNP[22].

23 The relationship between many diseases and transcription factors has led to tremendous interest
24 in global investigations of transcription factor activity. To decipher transcription factor activity requires
25 understanding the two major functions of a transcription factor: binding to DNA and modification
26 of transcription. Transcription factors bind to specific DNA sequences, a TF recognition motif. A
27 number of techniques have been utilized to identify and characterize these recognition motifs[23].
28 However, because most genomic instances of the motif are not actually bound, having the recognition
29 motif is insufficient. Protein-DNA interactions can be measured genome wide using chromatin
30 immunoprecipitation followed by sequencing (ChIP-seq)[23–25]. Unfortunately, numerous lines of
31 evidence indicate that not all binding events influence transcription[26–28]. Conceptually, this is akin
32 to saying that just because someone is standing in a lab (TF binding) it does not imply they are actually
33 conducting an experiment (altering transcription). Therefore, distinct assays are necessary to identify
34 the locations where a TF is bound to DNA and determine whether that DNA binding leads to altered
35 transcription nearby. A number of high throughput assays are available to interrogate these two key
36 functions.

37 Extensive attention has focused on determining where in the genome transcription factors bind[23,
38 29,30]. The ENCODE project alone included approximately 2000 TF ChIP-seq experiments, including
39 180 TFs in K562 (myeloid leukemia) cells alone[29]. Large regulation project such as ENCODE and
40 Roadmap Epigenomics have been invaluable to our understanding of TF binding. However, there are
41 an estimate 1600 TFs in the human genome and many do not have a reliable antibody for ChIP-seq[23].
42 Even when antibodies are available, individual transcription factors can have distinct profiles of
43 binding locations across cell types and conditions. Consequently, the cost of individually profiling
44 every TF in each cell type is enormous, much less across different conditions[31]. Finally, if the effect
45 of a particular perturbation is unknown, profiling assorted TFs by ChIP is prohibitively expensive.

46 An alternative approach to detecting individual protein-DNA binding locations is to infer a large
47 collection of binding events via DNA footprinting[32–34]. Dense mapping of DNase I cleavage sites
48 identifies small regions protected from cleavage by the presence of a bound transcription factor[32,33].
49 While early footprinting studies identified a large repertoire of previously un-characterized motifs
50 protected from cleavage, suggesting many novel transcription factors[34], subsequent work indicates
51 these regions likely reflect sequence based cleavage bias of the DNase I enzyme[35]. Additionally, it
52 is also now clear that most TFs (80%) do not show a measurable footprint[36], thereby limiting the
53 effectiveness of this approach.

54 Despite these limitations, DNA footprinting assays uncovered a distinct function for transcription
55 factors: altering DNA accessibility. When chromatin accessibility data is considered in the context of
56 known TF sequence motifs[37–40], one can reasonably infer transcription factor binding profiles[41,42].
57 When accessibility profiles are then compared to ChIP in the context of perturbations, transcription
58 factors could be classified as “pioneer” or “settler” depending on whether they open chromatin or
59 require accessible, exposed DNA to bind[42]. Whether alterations of local chromatin accessibility
60 reflect a byproduct of the TF’s DNA binding or its altering of transcription remains unclear.

61 Altering transcription is the second major function of transcription factors[23]. Because TFs
62 alter transcription, some of the earliest studies of TFs as regulators were based on expression data.
63 For nearly twenty years large compendiums of expression data have been utilized to infer gene
64 regulatory networks[43,44]. Typically these approaches search for modules, collections of co-regulated
65 genes across distinct conditions. Identification of nearby TF recognition motifs[45,46] or co-regulated
66 transcription factors[43] link particular TFs to the module of genes they regulate. For instance, ISMARA
67 (Integrated System for Motif Activity Response Analysis)[47] models gene expression in terms of TF
68 sequence motifs within proximal promoters. Gene regulatory network methods have been instrumental
69 for understanding large scale regulatory networks, but are inherently limited by the fact that they

70 depend on steady state expression data. Steady state expression assays (microarray or RNA-seq)
71 reflect not only transcription but also RNA processing, maturation and stability. Hence, they are an
72 indirect readout on the effect of perturbations to transcription factors. Additionally, they are generally
73 incapable of reliably detecting small changes at short time points without an impractical number of
74 replicates[48].

75 Nascent transcription assays (GRO-seq, PRO-seq) directly profile RNA associated with engaged
76 cellular polymerases[49,50]. Consequently, nascent assays are a direct readout on changes to
77 transcription induced by perturbations[21,51]. Interestingly, an additional feature of nascent
78 transcription data is the identification of short unstable transcripts immediately proximal to sites
79 of transcription factor binding[52–57]. Importantly, these transcripts, now known as eRNAs can be
80 employed as markers of TF activity[58]. The change in patterns of eRNA usage genome-wide relative to
81 TF recognition motifs allows one to determine which transcription factors are altered by a perturbation
82 with no a priori information. Unfortunately, nascent transcription protocols[49,50] are onerous, time
83 consuming, and require large numbers of cells as input. Consequently, these experimental assays are
84 predominantly used on cultured cell lines and not yet widely adopted. Therefore, we sought a simpler,
85 easy to use approach to inferring differential transcription factor activity.

86 The Assay for Transposase-Accessible Chromatin followed by sequencing (ATAC-seq), a method
87 for identifying regions of open chromatin, is particularly attractive because it is quick, easy, inexpensive,
88 and deployable in small cell count samples. Additionally, recent work has shown that changes in
89 chromatin accessibility can inform on TF activity. Specifically, BagFoot[36] combined footprinting
90 with differential accessibility to identify TFs associated with altered chromatin accessibility profiles
91 in the presence of a perturbation. They predominantly focused on DNase I hypersensitivity data,
92 but also examined a small number of ATAC-seq datasets. Here we seek to confirm and extend their
93 results in two ways. First, we ask whether an alternative approach – namely the motif displacement
94 statistic[58], developed initially for nascent transcription analysis, could infer differential TF activity
95 from ATAC-seq datasets. Second, we sought to construct an easy-to-use pipeline specific to the analysis
96 of differential ATAC-seq analysis.

97 2. Results

98 We introduce a tool, Differential ATAC-seq toolkit (DAStk), developed with simplicity and ease of
99 implementation in mind, focused around inferring changes in TF activity from ATAC-seq data. Using
100 nascent transcription data we had previously developed the motif displacement score (MD-score) a
101 metric that assesses TF associated transcriptional activity. As such, the MD-score reflects the enrichment
102 of TF sequence motif within an small radius (150 bp) of enhancer RNA (eRNA) origins relative to a
103 larger local window (1500 bp)[58]. While ATAC-seq does not directly provide information on eRNAs,
104 most sites of eRNA activity reside within open chromatin[59]. Therefore we utilize the midpoint of
105 called ATAC-seq peaks (rather than the eRNA origin) as a frame of reference for calculating MD-scores.
106 Then, given two distinct biological conditions, we compare the ratio of MD-scores across the conditions
107 and identify statistically significant changes by a two-proportion Z-test. Using public ATAC-seq data
108 from a variety of human and mouse cell lines (IMR90, H524, NJH29, ZHBTC4) and perturbations
109 (nutlin, doxycycline, tamoxifen), we assessed changes in accessibility over all putative TF sequence
110 recognition motifs (for all motifs within the HOCOMOCO database[38]).

111 Given our familiarity with TP53 activation[55,60], we first examined this approach on ATAC-seq
112 data gathered before and 6 hours after Nutlin-3a exposure on IMR90 cells[61]. Nutlin-3a is an
113 exquisitely specific activator of TP53. As expected, we found that TP53 displayed the most significant
114 change (p -value $< 10^{-5}$) in MD-score (Figure 1A, in red) of all motifs within the HOCOMOCO
115 database[38]. Relaxing the p -value cutoff (p -value $< 10^{-4}$) we subsequently identified altered activity
116 in TP63 and TP73 (Figure 1A, in maroon), likely reflecting the fact that these two proteins have nearly
117 identical sequence recognition motifs as TP53.

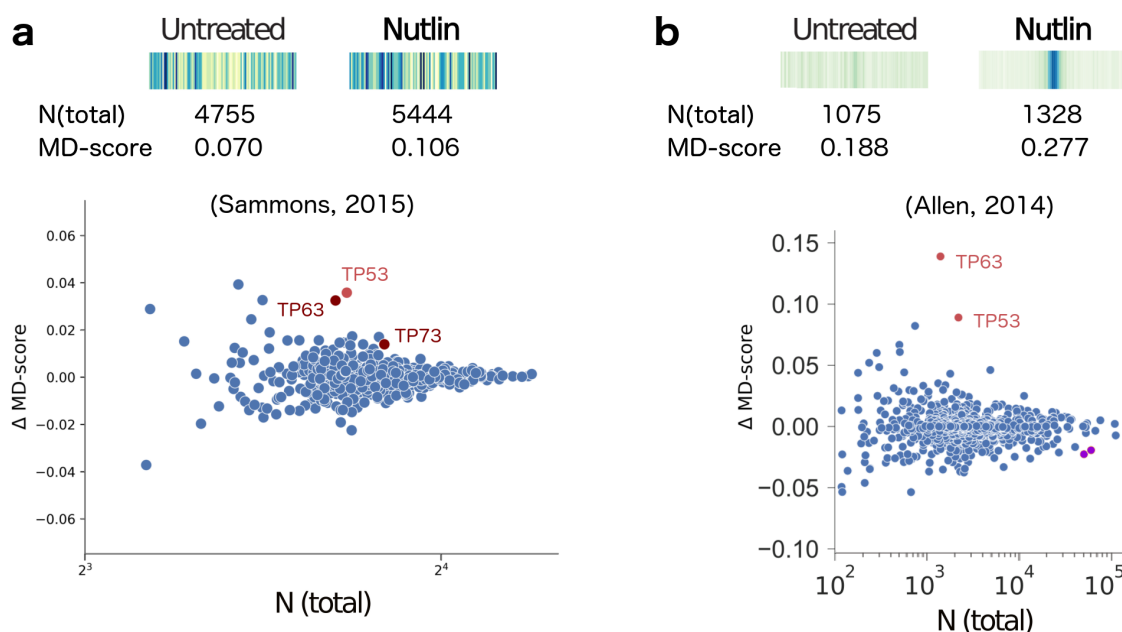


Figure 1. (a)Top: The motif displacement distribution as heatmap (increasingly dark blue indicates more instances of motif), MD-score and the number of motifs within 1.5kb of an ATAC-seq peak before and after stimulation with Nutlin-3a (e.g. Nutlin)[61] for TP53, the transcription factor known to be activated. Bottom: For all motif models (each dot), the change in MD-score following perturbation (y-axis) relative to the number of motifs within 1.5kb of any ATAC-seq peak center (x-axis). Red/maroon points indicate significantly increased MD-scores (p-value < 10^{-5} , < 10^{-4} , respectively). (b) Similar analysis obtained from nascent transcription data[55], where MD-scores are measured relative to eRNA origins. Purple dots indicate significantly decreased MD-scores. Figure adapted from Azofeifa et al [58].

118 Interestingly, Nutlin-3a has also been analyzed using nascent transcription data albeit in a different
119 cell line (HCT116) at a shorter time point (1 hour)[55]. The MD-score analysis of the nascent data[58]
120 obtained very similar results (Figure 1B). Unfortunately, a direct comparison of individual genomic
121 loci between the two data sets is not feasible because they used different cell lines and drug exposure
122 times. However, a couple of interesting observations concerning the overall MD-score trends are
123 none-the-less noteworthy. First, the co-localization of the TP53 motif with ATAC-peak midpoints is
124 far less striking than the co-localization of motifs with the eRNA origins (observed in the heatmap
125 histograms). This observation, combined with the relative lower magnitude of Δ MD-scores (y-axis)
126 suggests that the eRNA origin (obtained in nascent transcription) is a far more precise method of
127 localizing and detecting changes in TF activity. Second, despite this lack of precision, ATAC-seq
128 correctly identifies TP53 as the most dramatically altered MD-score whereas the best scoring motif with
129 nascent transcription is TP63. Why this discrepancy exists is unclear, but given the relative similarity
130 of these two motifs it may simply be coincidental.

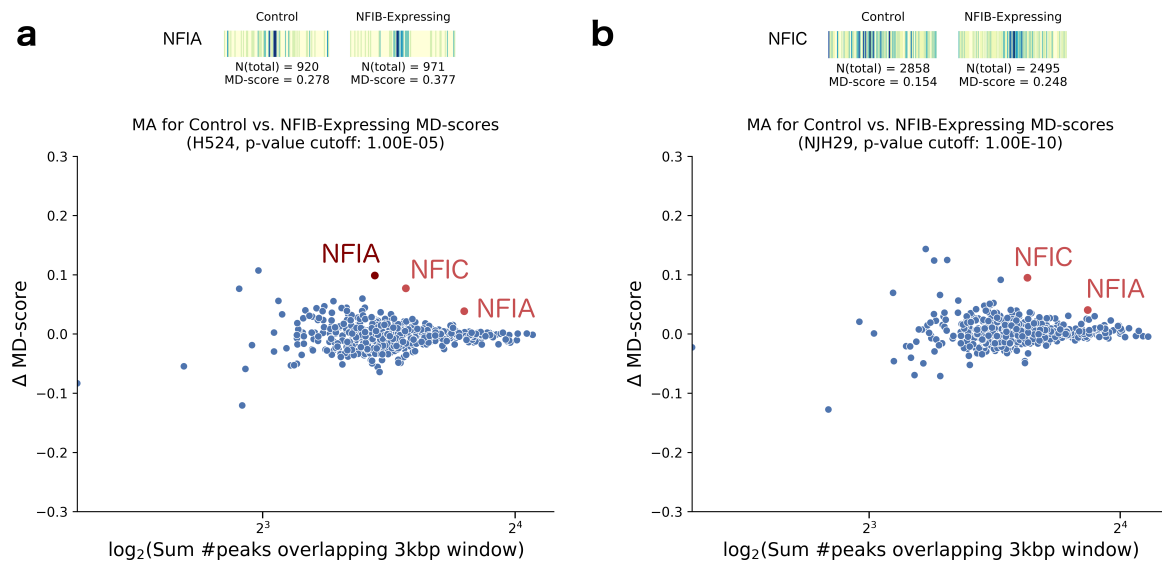


Figure 2. (a) Top: Motif displacement distribution as heatmap (increasingly dark blue indicates more instances of motif), MD-score and the number of motifs within 1.5kb of an ATAC-seq peak in control and NFIB-induced H524 cells with doxycycline, for the upregulated TF NFIA. Bottom: For all motif models (each dot), the change in MD-score following perturbation (y-axis) relative to the number of motifs within 1.5kb of any ATAC-seq peak center (x-axis). Red/maroon points indicate significantly increased MD-scores (p -value $< 10^{-5}$, $< 10^{-4}$, respectively). (b) Equivalent analysis performed on NJH29 cells, displaying a motif displacement distribution of the NFIC TF upregulation. We note that in the doxycycline-treated cells, most ATAC-seq peaks are located closer to the motif center than on the control cells.

131 We next analyzed differential ATAC-data gathered by Denny et. al to examine whether Nfib
132 promotes metastasis via increasing chromatin accessibility. For this question, they examined two
133 human small cell lung carcinoma (SCLC) cell lines (H524 and NJH29), profiling by ATAC-seq before
134 and four hours after doxycycline treatment. Using the MD-score approach, we detect changes in TF
135 activity for multiple members of the NFI family (Figure 2A,B). An increase in NFIA (two different
136 motifs) and NFIC was detected in both cell types (p -value $< 10^{-5}$ for H524s; p -value $< 10^{-10}$ for
137 NJH29s). As further confirmation of the NFI signal, we tested one of their mouse samples (KP22 cells)
138 and found an increase of NFIA (p -value $< 10^{-5}$), consistent with the human results. We next asked
139 whether our results were sensitive to the particular peaks utilized. To this end we sub-sampled peaks
140 from the NJH29 data and re-ran our analysis. Both NFIA and NFIC are detectable as significant (p -value
141 $< 10^{-10}$) even when using only half of the ATAC-seq peaks, suggesting the signal is reasonably robust.

142 We then sought to determine how the Δ MD-score approach compared to the BagFoot[36] at
143 identifying differential TF activity. BagFoot also identified NIFA and NIFC within the SCLC differential
144 ATAC-seq data[36]. However, they additionally claimed HNF6 as potentially altered in the SCLC
145 data. Importantly, Baek et. al. noted that the HNF6 result did not hold when their approach utilized
146 bias corrected data (based on naked DNA digested with Tn5). Given our MD-score approach does
147 not identify HNF6 as altered further supports the idea that this result reflects a data artifact rather
148 than a true biological phenomena. Interestingly, the MD-score approach and Bagfoot obtained nearly
149 identical results on a second differential ATAC-seq dataset. In this case, King and Klose[62] showed
150 BRG1, essential for pluripotency-related chromatin modifications, is required to make chromatin
151 accessible at OCT4 target sites. To this end they treated ZHBTC4 mouse embryonic stem cells (ESCs)
152 with tamoxifen for 72 hours to block BRG1 expression. When compared to the unperturbed mouse ESC
153 control, we observed lowered MD-scores for SOX2, PO5F1 (Oct4) and NANOG in the BRG1-blocked
154 cells (p -value $< 10^{-13}$; Figure 3A), directly confirming the BagFoot findings.

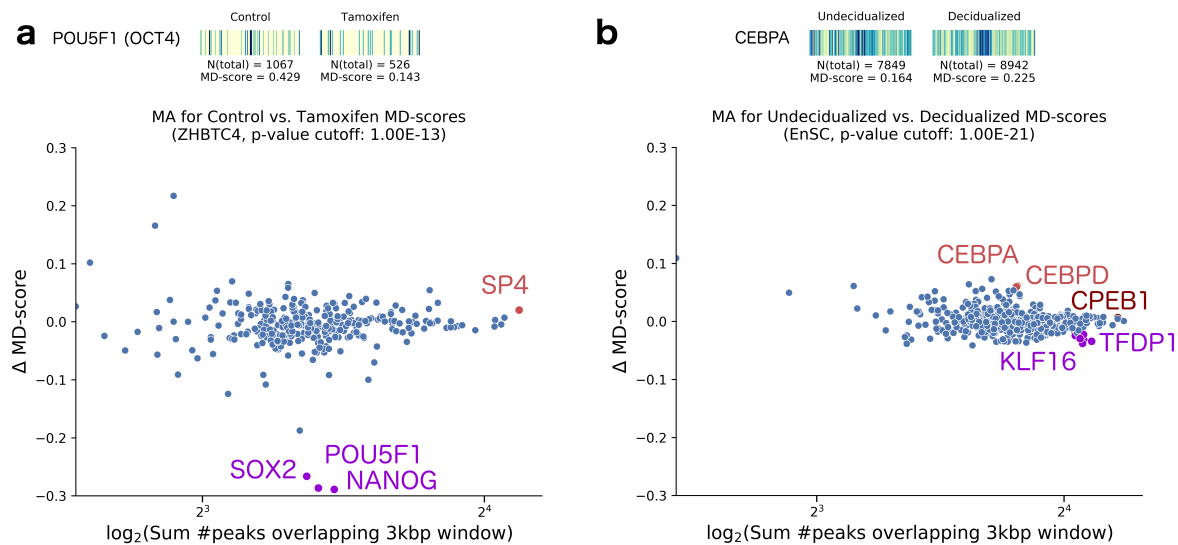


Figure 3. (a) Top: Motif displacement distribution as heatmap (increasingly dark blue indicates more instances of motif), MD-score and the number of motifs within 1.5kb of an ATAC-seq peak before and after stimulation with Tamoxifen[62] for the inhibited TF POU5F1, also known as OCT4. We observe that the decreased MD-score reflects not only a smaller number of peaks nearby this motif, but also a sharp decrease in co-localization with the motif. Bottom: For all motif models (each dot), the change in MD-score following perturbation (y-axis) relative to the number of motifs within 1.5kb of any ATAC-seq peak center (x-axis). Red points indicate significantly increased MD-scores (p-value < 10⁻¹³). Purple dots indicate significantly decreased MD-scores, at the same indicated p-value. (b) Equivalent analysis performed on endometrial stromal cells, before and after undergoing a decidualization process[63]. The motif displacement heatmap illustrates ATAC-seq peak distances to CEBPA, the TF expected to be upregulated.

155 Finally, we also examined a differential ATAC-seq data obtained for decidualized and
 156 undecidualized human endometrium cells[63]. Spontaneous decidualization occurs in response
 157 to progesterone signalling (i.e. by an implanted embryo at the early stages of pregnancy). Using
 158 our MD-score approach, we found the CEBP family of transcription factors had increased activity in
 159 decidualized cells, consistent with the author's conclusion (Figure 3B). Additionally, we also found
 160 significantly lowered MD-scores for the KLF16 motif (a TF known to be involved in regulatory uterine
 161 cell biology[64]) and TFDP1 (a known target to the estrogen receptor *ER* β present in all endometrial
 162 cell types[65] of lower activity during the secretory phase, in concert with the decidualization process).
 163 In all cases, the magnitude of MD-score alterations were relatively small, and yet the transcription
 164 factors uncovered can be linked to the underlying decidualization process.

165 3. Discussion

166 We sought to identify changes in TF activity across differential ATAC-seq datasets, as this protocol
 167 is inexpensive, simple and requires relatively small cell counts. Here we demonstrate two important
 168 results. First, using a simple statistic (the motif displacement score) as a co-localization measure of
 169 ATAC-seq peak midpoints to TF sequence motif sites across the genome, we correctly detect changes
 170 in TF activity. Second, our approach independently confirms the results obtained by BagFoot[36],
 171 as the two analysis techniques are distinct in their approach to quantifying differences in chromatin
 172 accessibility across conditions. Arguably, regardless of which analysis technique is preferred —
 173 differential ATAC-seq is a relatively simple and inexpensive way to assess for changes in TF activity
 174 induced by perturbations.

175 We believe there are two distinct advantages to the MD-score approach to assessing TF activity.
 176 First, the MD-score is calculated relative to a local background window. Consequently it cleanly

177 accounts for the localized sequence bias observed at promoters and enhancers[58], which likely reduces
178 false positives. Second, the statistic is relatively simple to implement and naturally accommodates
179 multiprocessing for faster computations. DASTk can easily be incorporated at the tail-end of a
180 traditional processing pipeline for ATAC-seq data, in that MD-scores are calculated directly from called
181 peaks and genomic sequence.

182 Our MD-score statistic was originally developed for analysis of nascent transcription data[58]
183 and focused on enhancer RNA co-localization with motifs. Given most eRNAs originate from areas
184 of open chromatin[21,57,66] and many transcription factors can alter chromatin accessibility[42], it
185 is perhaps unsurprising that differential chromatin accessibility can be used to infer changes in TF
186 activity. However, it remains unclear whether the observed alterations of chromatin reflect a distinct
187 functional activity of transcription factors or are simply a side effect of DNA binding and/or altering
188 transcription. While a careful examination of the two Nutlin-3a datasets (Figure 1) identifies several
189 genomic regions altered uniquely in only one of the two datasets (ATAC-seq or nascent), the lack of
190 matched data makes interpretation of these differences difficult. Do they reflect differences of cell type
191 or distinct functional activities of TP53? A careful comparison of chromatin accessibility and nascent
192 transcription data in the context of a perturbation will be necessary to fully address this question.

193 4. Materials and Methods

194 4.1. Processing pipeline

195 Each ATAC-seq dataset was subjected to a standard data processing pipeline. The SRR datasets
196 were converted to FASTQ format using `fastq-dump v2.8.0` with argument `-split-3`. Paired-ended
197 raw reads were trimmed using `trimmomatic v0.36` at a fixed length with options `PE -phred33`
198 `CROP:36 HEADCROP:6`. After verifying the dataset quality with `FastQC v0.11.5`, the reads were aligned
199 to the hg19 or mm10 reference genome, using `Bowtie v2.2.9` with arguments `-p32 -X2000`. The
200 resulting SAM files were converted to BAM format using `samtools v1.3.1` using the view `-q 20 -S`
201 `-b` arguments and sorted with the `sort -m500G` arguments. Bam files were then converted to BedGraph
202 format for easier processing using `bedtools v2.25.0` with arguments `-bg -ibam INPUT_BAM_FILE`
203 `-g GENOME_REFERENCE` and read counts were normalized by the millions mapped. Finally, `MACS`
204 `v2.1.1.20160309` was used to call broad peaks from the ATAC-seq BAM files with arguments `callpeak`
205 `-n ASSAY_PREFIX -nomodel -format BAMPE -shift -100 -extsize 200 -B -broad`.

206 The human motif sites calculated in Azofeifa et al[58] for the hg19 reference genome were used
207 for human cells. The motif sites for mouse cells were obtained using `FIMO` with position weight
208 matrices (PWMs) from `HOCOMOCO`, with a p-value cutoff of 10^{-6} (arguments `-max-stored-scores`
209 `10000000 -thresh 1e-6`).

210 4.2. Public Datasets

211 We used samples from the following public GEO datasets for our analysis: GSE58740
212 (samples SRR1448793 and SRR1448795), GSE81255/GSE81258 (samples SRR3493647, SRR3493653,
213 SRR3493643, SRR3493645, SRR3493626, SRR3493627, SRR3493634, and SRR3493635), GSE87822
214 (samples SRR4413799 and SRR4413811), and GSE104720 (samples SRR6148318 and SRR6148319).

215 4.3. DASTk Software

216 The Differential ATAC-seq toolkit (DASTk) is a collection of scripts publicly available at
217 <https://biof-git.colorado.edu/dowelllab/DASTk> for download. We used 642 PWMs of human motifs
218 in the `HOCOMOCO`[38] database (to verify the presence of ATAC-seq peaks nearby), and 427 mouse
219 motifs. TF sequence motifs were mapped to the hg19 or mm10 reference genomes with a p-value cutoff
220 of 10^{-6} . For each motif, the number of ATAC-seq peaks was accounted for, within a large (1500bp
221 radius) and small (150bp radius) window, to calculate the motif displacement score. The difference
222 between the MD-score in each condition and the number of ATAC-seq peaks nearby (large window)

223 each motif were used to produce the MA plots. Those motifs with a statistically significant difference
224 in MD-score were labeled, as determined by a z-test of two proportions[58].

225 **Acknowledgments:** This work was funded in part by a NSF IGERT grant number 1144807 (IJT, RDD), NIH
226 training grant T15LM009451 (IJT), a Sie Fellowship (MAA) and a NSF ABI DBI-12624L0 (RDD). The authors
227 acknowledge the BioFrontiers Computing Core at the University of Colorado Boulder for providing High
228 Performance Computing resources (NIH 1S10OD012300) supported by BioFrontiers' IT.

229 **Author Contributions:** MAA and RDD conceived and designed the experiments; IJT implemented DASTk and
230 performed the experiments; IJT and RDD analyzed the data; all authors contributed to writing the paper.

231 **Conflicts of Interest:** The authors declare no conflict of interest. The founding sponsors had no role in the design
232 of the study; in the collection, analyses, or interpretation of data; in the writing of the manuscript, and in the
233 decision to publish the results.

234 Abbreviations

235 The following abbreviations are used in this manuscript:

236 TF	Transcription factor
ATAC	Assay for Transposase-Accessible Chromatin
SNP	single nucleotide polymorphisms
237 ChIP	chromatin immunoprecipitation
eRNA	enhancer RNA
MD-score	motif displacement score
SCLC	small cell lung carcinoma

238 References

- 239 1. Spitz, F.; Furlong, E.E.M. Transcription factors: from enhancer binding to developmental control. *Nat Rev*
240 *Genet* **2012**, *13*, 613–626.
- 241 2. Latchman, D.S. Transcription-Factor Mutations and Disease. *New England Journal of Medicine* **1996**,
242 *334*, 28–33.
- 243 3. Muller, P.A.J.; Vousden, K.H. p53 mutations in cancer. *Nat Cell Biol* **2013**, *15*, 2–8.
- 244 4. Jongmans, M.C.J.; Kuiper, R.P.; Carmichael, C.L.; Wilkins, E.J.; Dors, N.; Carmagnac, A.; Schouten-van
245 Meeteren, A.Y.N.; Li, X.; Stankovic, M.; Kamping, E.; Bengtsson, H.; Schoenmakers, E.F.P.M.; van
246 Kessel, A.G.; Hoogerbrugge, P.M.; Hahn, C.N.; Brons, P.P.; Scott, H.S.; Hoogerbrugge, N. Novel RUNX1
247 mutations in familial platelet disorder with enhanced risk for acute myeloid leukemia: clues for improved
248 identification of the FPD/AML syndrome. *Leukemia* **2009**, *24*, 242–246.
- 249 5. Leslie, E.J.; Liu, H.; Carlson, J.C.; Shaffer, J.R.; Feingold, E.; Wehby, G.; Laurie, C.A.; Jain, D.; Laurie, C.C.;
250 Doheny, K.F.; McHenry, T.; Resick, J.; Sanchez, C.; Jacobs, J.; Emanuele, B.; Vieira, A.R.; Neiswanger, K.;
251 Standley, J.; Czeizel, A.E.; Deleyiannis, F.; Christensen, K.; Munger, R.G.; Lie, R.T.; Wilcox, A.; Romitti, P.A.;
252 Field, L.L.; Padilla, C.D.; Cutionco-de la Paz, E.M.C.; Lidral, A.C.; Valencia-Ramirez, L.C.; Lopez-Palacio,
253 A.M.; Valencia, D.R.; Arcos-Burgos, M.; Castilla, E.E.; Mereb, J.C.; Poletta, F.A.; Orioli, I.M.; Carvalho,
254 F.M.; Hecht, J.T.; Blanton, S.H.; Buxó, C.J.; Butali, A.; Mossey, P.A.; Adeyemo, W.L.; James, O.; Braimah,
255 R.O.; Aregbesola, B.S.; Eshete, M.A.; Deribew, M.; Koruyucu, M.; Seymen, F.; Ma, L.; de Salamanca, J.E.;
256 Weinberg, S.M.; Moreno, L.; Cornell, R.A.; Murray, J.C.; Marazita, M.L. A Genome-wide Association Study
257 of Nonsyndromic Cleft Palate Identifies an Etiologic Missense Variant in GRHL3. *The American Journal of*
258 *Human Genetics* **2016**, *98*, 744–754.
- 259 6. Smith, S.; Kelley, P.; Kenyon, J.; Hoover, D. Tietz syndrome (hypopigmentation/deafness) caused by
260 mutation of MITF. *Journal of Medical Genetics* **2000**, *37*, 446–448.
- 261 7. Tassabehji, M.; Newton, V.E.; Read, A.P. Waardenburg syndrome type 2 caused by mutations in the human
262 microphthalmia (MITF) gene. *Nat Genet* **1994**, *8*, 251–255.
- 263 8. Marini, M.; Bocciardi, R.; Gimelli, S.; Di Duca, M.; Divizia, M.T.; Baban, A.; Gaspar, H.; Mammi, I.; Garavelli,
264 L.; Cerone, R.; Emma, F.; Bedeschi, M.F.; Tenconi, R.; Sensi, A.; Salmaggi, A.; Bengala, M.; Mari, F.; Colussi,
265 G.; Szczaluba, K.; Antonarakis, S.E.; Seri, M.; Lerone, M.; Ravazzolo, R. A spectrum of LMX1B mutations in
266 Nail-Patella syndrome: New point mutations, deletion, and evidence of mosaicism in unaffected parents.
267 *Genet Med* **2010**, *12*, 431–439.

- 268 9. Stiles, A.R.; Simon, M.T.; Stover, A.; Eftekharian, S.; Khanlou, N.; Wang, H.L.; Magaki, S.; Lee, H.;
269 Partynski, K.; Dorrani, N.; Chang, R.; Martinez-Agosto, J.A.; Abdenur, J.E. Mutations in TFAM, encoding
270 mitochondrial transcription factor A, cause neonatal liver failure associated with mtDNA depletion.
271 *Molecular Genetics and Metabolism* **2016**, *119*, 91–99.
- 272 10. Chung, I.M.; Rajakumar, G. Genetics of Congenital Heart Defects: The NKX2-5 Gene, a Key Player. *Genes*
273 **2016**, *7*, 6.
- 274 11. Yi Li, Q.; Newbury-Ecob, R.A.; Terrett, J.A.; Wilson, D.I.; Curtis, A.R.J.; Ho Yi, C.; Gebuhr, T.; Bullen, P.J.;
275 Robson, S.C.; Strachan, T.; Bonnet, D.; Lyonnet, S.; Young, I.D.; Raeburn, J.A.; Buckler, A.J.; Law, D.J.; Brook,
276 J.D. Holt-Oram syndrome is caused by mutations in TBX5, a member of the Brachyury (T) gene family.
277 *Nat Genet* **1997**, *15*, 21–29.
- 278 12. Narumi, Y.; Nishina, S.; Tokimitsu, M.; Aoki, Y.; Kosaki, R.; Wakui, K.; Azuma, N.; Murata, T.; Takada, F.;
279 Fukushima, Y.; Kosho, T. Identification of a novel missense mutation of MAF in a Japanese family with
280 congenital cataract by whole exome sequencing: A clinical report and review of literature. *American Journal*
281 *of Medical Genetics Part A* **2014**, *164*, 1272–1276.
- 282 13. Sweatt, J.D. Pitt-Hopkins Syndrome: intellectual disability due to loss of TCF4-regulated gene transcription.
283 *Exp Mol Med* **2013**, *45*, e21.
- 284 14. Lee, T.I.; Young, R.A. Transcriptional Regulation and Its Misregulation in Disease. *Cell* **2013**, *152*, 1237 –
285 1251.
- 286 15. Maurano, M.T.; Haugen, E.; Sandstrom, R.; Vierstra, J.; Shafer, A.; Kaul, R.; Stamatoyannopoulos, J.A.
287 Large-scale identification of sequence variants influencing human transcription factor occupancy in vivo.
288 *Nature Genetics* **2015**, *47*, 1393–1401.
- 289 16. Shlyueva, D.; Stampfel, G.; Stark, A. Transcriptional enhancers: from properties to genome-wide
290 predictions. *Nat Rev Genet* **2014**, *15*, 272–286.
- 291 17. Maurano, M.T.; Humbert, R.; Rynes, E.; Thurman, R.E.; Haugen, E.; Wang, H.; Reynolds, A.P.; Sandstrom,
292 R.; Qu, H.; Brody, J.; Shafer, A.; Neri, F.; Lee, K.; Kutayavin, T.; Stehling-Sun, S.; Johnson, A.K.; Canfield, T.K.;
293 Giste, E.; Diegel, M.; Bates, D.; Hansen, R.S.; Neph, S.; Sabo, P.J.; Heimfeld, S.; Raubitschek, A.; Ziegler,
294 S.; Cotsapas, C.; Sotoodehnia, N.; Glass, I.; Sunyaev, S.R.; Kaul, R.; Stamatoyannopoulos, J.A. Systematic
295 Localization of Common Disease-Associated Variation in Regulatory DNA. *Science* **2012**, *337*, 1190–1195.
- 296 18. Corradin, O.; Scacheri, P.C. Enhancer variants: evaluating functions in common disease. *Genome Medicine*
297 **2014**, *6*, 85.
- 298 19. Mifsud, B.; Tavares-Cadete, F.; Young, A.N.; Sugar, R.; Schoenfelder, S.; Ferreira, L.; Wingett, S.W.; Andrews,
299 S.; Grey, W.; Ewels, P.A.; Herman, B.; Happe, S.; Higgs, A.; LeProust, E.; Follows, G.A.; Fraser, P.; Luscombe,
300 N.M.; Osborne, C.S. Mapping long-range promoter contacts in human cells with high-resolution capture
301 Hi-C. *Nat Genet* **2015**, *47*, 598–606.
- 302 20. Farh, K.K.H.; Marson, A.; Zhu, J.; Kleinewietfeld, M.; Housley, W.J.; Beik, S.; Shores, N.; Whitton, H.;
303 Ryan, R.J.H.; Shishkin, A.A.; Hatan, M.; Carrasco-Alfonso, M.J.; Mayer, D.; Luckey, C.J.; Patsopoulos, N.A.;
304 De Jager, P.L.; Kuchroo, V.K.; Epstein, C.B.; Daly, M.J.; Hafler, D.A.; Bernstein, B.E. Genetic and epigenetic
305 fine mapping of causal autoimmune disease variants. *Nature* **2015**, *518*, 337–343.
- 306 21. Lam, M.T.; Li, W.; Rosenfeld, M.G.; Glass, C.K. Enhancer {RNAs} and regulated transcriptional programs.
307 *Trends in Biochemical Sciences* **2014**, *39*, 170 – 182.
- 308 22. Ward, L.D.; Kellis, M. HaploReg: a resource for exploring chromatin states, conservation, and regulatory
309 motif alterations within sets of genetically linked variants. *Nucleic Acids Research* **2011**, *40*, D930.
- 310 23. Lambert, S.A.; Jolma, A.; Campitelli, L.F.; Das, P.K.; Yin, Y.; Albu, M.; Chen, X.; Taipale, J.; Hughes, T.R.;
311 Weirauch, M.T. The Human Transcription Factors. *Cell* **2018**, *172*, 650–665.
- 312 24. Farnham, P.J. Insights from genomic profiling of transcription factors. *Nat Rev Genet* **2009**, *10*, 605–616.
- 313 25. Gade, P.; Kalvakolanu, D.V. Chromatin Immunoprecipitation Assay as a Tool for Analyzing Transcription
314 Factor Activity. *Methods in molecular biology (Clifton, N.J.)* **2012**, *809*, 85–104.
- 315 26. Whitfield, T.W.; Wang, J.; Collins, P.J.; Partridge, E.C.; Aldred, S.F.; Trinklein, N.D.; Myers, R.M.; Weng, Z.
316 Functional analysis of transcription factor binding sites in human promoters. *Genome Biology* **2012**, *13*, R50.
- 317 27. Spivakov, M. Spurious transcription factor binding: Non-functional or genetically redundant? *BioEssays*
318 **2014**, *36*, 798–806.
- 319 28. Cusanovich, D.A.; Pavlovic, B.; Pritchard, J.K.; Gilad, Y. The Functional Consequences of Variation in
320 Transcription Factor Binding. *PLoS Genet* **2014**, *10*, e1004226.

- 321 29. The ENCODE Project Consortium. An integrated encyclopedia of DNA elements in the human genome.
322 *Nature* **2012**, *489*, 57–74.
- 323 30. Consortium, R.E.; Kundaje, A.; Meuleman, W.; Ernst, J.; Bilenky, M.; Yen, A.; Heravi-Moussavi, A.;
324 Kheradpour, P.; Zhang, Z.; Wang, J.; Ziller, M.J.; Amin, V.; Whitaker, J.W.; Schultz, M.D.; Ward, L.D.; Sarkar,
325 A.; Quon, G.; Sandstrom, R.S.; Eaton, M.L.; Wu, Y.C.; Pfennig, A.R.; Wang, X.; Claussnitzer, M.; Liu, Y.;
326 Coarfa, C.; Harris, R.A.; Shores, N.; Epstein, C.B.; Gjoneska, E.; Leung, D.; Xie, W.; Hawkins, R.D.; Lister,
327 R.; Hong, C.; Gascard, P.; Mungall, A.J.; Moore, R.; Chuah, E.; Tam, A.; Canfield, T.K.; Hansen, R.S.; Kaul,
328 R.; Sabo, P.J.; Bansal, M.S.; Carles, A.; Dixon, J.R.; Farh, K.H.; Feizi, S.; Karlic, R.; Kim, A.R.; Kulkarni, A.; Li,
329 D.; Lowdon, R.; Elliott, G.; Mercer, T.R.; Neph, S.J.; Onuchic, V.; Polak, P.; Rajagopal, N.; Ray, P.; Sallari,
330 R.C.; Siebenthal, K.T.; Sinnott-Armstrong, N.A.; Stevens, M.; Thurman, R.E.; Wu, J.; Zhang, B.; Zhou, X.;
331 Beaudet, A.E.; Boyer, L.A.; De Jager, P.L.; Farnham, P.J.; Fisher, S.J.; Haussler, D.; Jones, S.J.M.; Li, W.; Marra,
332 M.A.; McManus, M.T.; Sunyaev, S.; Thomson, J.A.; Tlsty, T.D.; Tsai, L.H.; Wang, W.; Waterland, R.A.; Zhang,
333 M.Q.; Chadwick, L.H.; Bernstein, B.E.; Costello, J.F.; Ecker, J.R.; Hirst, M.; Meissner, A.; Milosavljevic,
334 A.; Ren, B.; Stamatoyannopoulos, J.A.; Wang, T.; Kellis, M.; Consortium, R.E. Integrative analysis of 111
335 reference human epigenomes. *Nature* **2015**, *518*, 317–330.
- 336 31. Steinhauser, S.; Kurzawa, N.; Eils, R.; Herrmann, C. A comprehensive comparison of tools for differential
337 ChIP-seq analysis. *Briefings in Bioinformatics* **2016**, *17*, 953–966.
- 338 32. Hesselberth, J.R.; Chen, X.; Zhang, Z.; Sabo, P.J.; Sandstrom, R.; Reynolds, A.P.; Thurman, R.E.; Neph,
339 S.; Kuehn, M.S.; Noble, W.S.; Fields, S.; Stamatoyannopoulos, J.A. Global mapping of protein-DNA
340 interactions in vivo by digital genomic footprinting. *Nature methods* **2009**, *6*, 283–289.
- 341 33. Chen, X.; Hoffman, M.M.; Bilmes, J.A.; Hesselberth, J.R.; Noble, W.S. A dynamic Bayesian network for
342 identifying protein-binding footprints from single molecule-based sequencing data. *Bioinformatics* **2010**,
343 *26*, i334–i342.
- 344 34. Neph, S.; Vierstra, J.; Stergachis, A.B.; Reynolds, A.P.; Haugen, E.; Vernot, B.; Thurman, R.E.; John, S.;
345 Sandstrom, R.; Johnson, A.K.; Maurano, M.T.; Humbert, R.; Rynes, E.; Wang, H.; Vong, S.; Lee, K.; Bates,
346 D.; Diegel, M.; Roach, V.; Dunn, D.; Neri, J.; Schafer, A.; Hansen, R.S.; Kutyaev, T.; Giste, E.; Weaver, M.;
347 Canfield, T.; Sabo, P.; Zhang, M.; Balasundaram, G.; Byron, R.; MacCoss, M.J.; Akey, J.M.; Bender, M.A.;
348 Groudine, M.; Kaul, R.; Stamatoyannopoulos, J.A. An expansive human regulatory lexicon encoded in
349 transcription factor footprints. *Nature* **2012**, *489*, 83–90.
- 350 35. He, H.H.; Meyer, C.A.; Hu, S.S.; Chen, M.W.; Zang, C.; Liu, Y.; Rao, P.K.; Fei, T.; Xu, H.; Long, H.; Liu,
351 X.S.; Brown, M. Refined DNase-seq protocol and data analysis reveals intrinsic bias in transcription factor
352 footprint identification. *Nature Methods* **2013**, *11*, 73 EP –.
- 353 36. Baek, S.; Goldstein, I.; Hager, G.L. Bivariate Genomic Footprinting Detects Changes in Transcription Factor
354 Activity. *Cell Reports* **2017**, *19*, 1710 – 1722.
- 355 37. Kulakovskiy, I.V.; Medvedeva, Y.A.; Schaefer, U.; Kasianov, A.S.; Vorontsov, I.E.; Bajic, V.B.; Makeev, V.J.
356 HOCOMOCO: a comprehensive collection of human transcription factor binding sites models. *Nucleic
357 Acids Research* **2013**, *41*, D195–D202.
- 358 38. Kulakovskiy, I.V.; Vorontsov, I.E.; Yevshin, I.S.; Sharipov, R.N.; Fedorova, A.D.; Rumynskiy, E.I.; Medvedeva,
359 Y.A.; Magana-Mora, A.; Bajic, V.B.; Papatsenko, D.A.; Kolpakov, F.A.; Makeev, V.J. HOCOMOCO: towards
360 a complete collection of transcription factor binding models for human and mouse via large-scale ChIP-Seq
361 analysis. *Nucleic Acids Research* **2018**, *46*, D252–D259.
- 362 39. Matys, V.; Kel-Margoulis, O.V.; Fricke, E.; Liebich, I.; Land, S.; Barre-Dirrie, A.; Reuter, I.; Chekmenev, D.;
363 Krull, M.; Hornischer, K.; Voss, N.; Stegmaier, P.; Lewicki-Potapov, B.; Saxel, H.; Kel, A.E.; Wingender, E.
364 TRANSFAC® and its module TRANSCompel®: transcriptional gene regulation in eukaryotes. *Nucleic
365 Acids Research* **2006**, *34*, D108–D110.
- 366 40. Portales-Casamar, E.; Thongjuea, S.; Kwon, A.T.; Arenillas, D.; Zhao, X.; Valen, E.; Yusuf, D.; Lenhard, B.;
367 Wasserman, W.W.; Sandelin, A. JASPAR 2010: the greatly expanded open-access database of transcription
368 factor binding profiles. *Nucleic Acids Research* **2010**, *38*, D105–D110.
- 369 41. Pique-Regi, R.; Degner, J.F.; Pai, A.A.; Gaffney, D.J.; Gilad, Y.; Pritchard, J.K. Accurate inference of
370 transcription factor binding from DNA sequence and chromatin accessibility data. *Genome Research* **2011**,
371 *21*, 447–455.

- 372 42. Sherwood, R.I.; Hashimoto, T.; O'Donnell, C.W.; Lewis, S.; Barkal, A.A.; van Hoff, J.P.; Karun, V.; Jaakkola,
373 T.; Gifford, D.K. Discovery of directional and nondirectional pioneer transcription factors by modeling
374 DNase profile magnitude and shape. *Nature biotechnology* **2014**, *32*, 171–178.
- 375 43. Segal, E.; Shapira, M.; Regev, A.; Pe'er, D.; Botstein, D.; Koller, D.; Friedman, N. Module networks:
376 identifying regulatory modules and their condition-specific regulators from gene expression data. *Nat*
377 *Genet* **2003**, *34*, 166–176.
- 378 44. Thompson, D.; Regev, A.; Roy, S. Comparative Analysis of Gene Regulatory Networks: From Network
379 Reconstruction to Evolution. *Annual Review of Cell and Developmental Biology* **2015**, *31*, 399–428.
- 380 45. Tavazoie, S.; Hughes, J.D.; Campbell, M.J.; Cho, R.J.; Church, G.M. Systematic determination of genetic
381 network architecture. *Nature Genetics* **1999**, *22*, 281 EP –.
- 382 46. Pilpel, Y.; Sudarsanam, P.; Church, G.M. Identifying regulatory networks by combinatorial analysis of
383 promoter elements. *Nature Genetics* **2001**, *29*, 153 EP –.
- 384 47. Balwiercz, P.J.; Pachkov, M.; Arnold, P.; Gruber, A.J.; Zavolan, M.; van Nimwegen, E. ISMARA: automated
385 modeling of genomic signals as a democracy of regulatory motifs. *Genome Research* **2014**.
- 386 48. Hart, S.N.; Therneau, T.M.; Zhang, Y.; Poland, G.A.; Kocher, J.P. Calculating Sample Size Estimates for
387 RNA Sequencing Data. *Journal of Computational Biology* **2013**, *20*, 970–978.
- 388 49. Core, L.J.; Waterfall, J.J.; Lis, J.T. Nascent RNA Sequencing Reveals Widespread Pausing and Divergent
389 Initiation at Human Promoters. *Science* **2008**, *322*, 1845–1848.
- 390 50. Kwak, H.; Fuda, N.J.; Core, L.J.; Lis, J.T. Precise Maps of RNA Polymerase Reveal How Promoters Direct
391 Initiation and Pausing. *Science (New York, N.Y.)* **2013**, *339*, 950–953.
- 392 51. Liu, Y.; Chen, S.; Wang, S.; Soares, F.; Fischer, M.; Meng, F.; Du, Z.; Lin, C.; Meyer, C.; DeCaprio, J.A.;
393 Brown, M.; Liu, X.S.; He, H.H. Transcriptional landscape of the human cell cycle. *Proceedings of the National*
394 *Academy of Sciences* **2017**, *114*, 3473–3478.
- 395 52. Kim, T.k.; Hemberg, M.; Gray, J.M.; Costa, A.M.; Bear, D.M.; Wu, J.; Harmin, D.A.; Laptewicz, M.;
396 Barbara-Haley, K.; Kuersten, S.; Markenscoff-Papadimitriou, E.; Kuhl, D.; Bito, H.; Worley, P.F.; Kreiman,
397 G.; Greenberg, M.E. Widespread transcription at neuronal activity-regulated enhancers. *Nature* **2010**,
398 *465*, 182–187.
- 399 53. Hah, N.; Murakami, S.; Nagari, A.; Danko, C.G.; Kraus, W.L. Enhancer transcripts mark active estrogen
400 receptor binding sites. *Genome Research* **2013**, *23*, 1210–1223.
- 401 54. Luo, X.; Chae, M.; Krishnakumar, R.; Danko, C.G.; Kraus, W.L. Dynamic reorganization of the AC16
402 cardiomyocyte transcriptome in response to TNF α signaling revealed by integrated genomic analyses.
403 *BMC Genomics* **2014**, *15*, 155–155.
- 404 55. Allen, M.A.; Mellert, H.; Dengler, V.; Andryzik, Z.; Guarnieri, A.; Freeman, J.A.; Luo, X.; Kraus, W.L.;
405 Dowell, R.D.; Espinosa, J.M. Global analysis of p53-regulated transcription identifies its direct targets and
406 unexpected regulatory mechanisms. *eLife* **2014**, *3*, e02200.
- 407 56. Puc, J.; Kozbial, P.; Li, W.; Tan, Y.; Liu, Z.; Suter, T.; Ohgi, K.A.; Zhang, J.; Aggarwal, A.K.; Rosenfeld, M.G.
408 Ligand-Dependent Enhancer Activation Regulated by Topoisomerase-I Activity. *Cell* **2015**, *160*, 367 – 380.
- 409 57. Danko, C.G.; Hyland, S.L.; Core, L.J.; Martins, A.L.; Waters, C.T.; Lee, H.W.; Cheung, V.G.; Kraus, W.L.; Lis,
410 J.T.; Siepel, A. Identification of active transcriptional regulatory elements from GRO-seq data. *Nat Meth*
411 **2015**, *12*, 433–438.
- 412 58. Azofeifa, J.G.; Allen, M.A.; Hendrix, J.R.; Read, T.; Rubin, J.D.; Dowell, R.D. Enhancer RNA profiling
413 predicts transcription factor activity. *Genome Research* **2018**, *28*, 334–344.
- 414 59. Azofeifa, J.G.; Dowell, R.D. A generative model for the behavior of RNA polymerase. *Bioinformatics* **2017**,
415 *33*, 227–234.
- 416 60. Azofeifa, J.G.; Allen, M.A.; Lladser, M.E.; Dowell, R.D. An Annotation Agnostic Algorithm for Detecting
417 Nascent RNA Transcripts in GRO-Seq. *IEEE/ACM Transactions on Computational Biology and Bioinformatics*
418 **2017**, *14*, 1070–1081.
- 419 61. Sammons, M.A.; Zhu, J.; Drake, A.M.; Berger, S.L. TP53 engagement with the genome occurs in
420 distinct local chromatin environments via pioneer factor activity. *Genome Research* **2015**, *25*, 179–188.
421 doi:10.1101/gr.181883.114.
- 422 62. King, H.W.; Klose, R.J. The pioneer factor OCT4 requires the chromatin remodeller BRG1 to support gene
423 regulatory element function in mouse embryonic stem cells. *eLife* **2017**, *6*, e22631.

- 424 63. Vrljicak, P.; Lucas, E.S.; Lansdowne, L.; Lucciola, R.; Muter, J.; Dyer, N.P.; Brosens, J.J.; Ott, S. Analysis
425 of chromatin accessibility in decidualizing human endometrial stromal cells. *The FASEB Journal* **0**,
426 0, fj.201701098R.
- 427 64. Daftary, G.S.; Lomberk, G.A.; Buttar, N.S.; Allen, T.W.; Grzenda, A.; Zhang, J.; Zheng, Y.; Mathison,
428 A.J.; Gada, R.P.; Calvo, E.; Iovanna, J.L.; Billadeau, D.D.; Prendergast, F.G.; Urrutia, R. Detailed
429 Structural-Functional Analysis of the Krüppel-like Factor 16 (KLF16) Transcription Factor Reveals Novel
430 Mechanisms for Silencing Sp/KLF Sites Involved in Metabolism and Endocrinology. *Journal of Biological*
431 *Chemistry* **2012**, *287*, 7010–7025.
- 432 65. Tamm, K.; Rõõm, M.; Salumets, A.; Metsis, M. Genes targeted by the estrogen and progesterone receptors
433 in the human endometrial cell lines HEC1A and RL95-2. *Reproductive Biology and Endocrinology* **2009**, *7*, 150.
- 434 66. Azofeifa, J.; Allen, M.A.; Lladser, M.E.; Dowell, R. FStitch: A Fast and Simple Algorithm for Detecting
435 Nascent RNA Transcripts. Proceedings of the 5th ACM Conference on Bioinformatics, Computational
436 Biology, and Health Informatics; ACM: New York, NY, USA, 2014; BCB '14, pp. 174–183.

437 © 2018 by the authors. Submitted to *Molecules* for possible open access publication under the terms and conditions
438 of the Creative Commons Attribution (CC BY) license (<http://creativecommons.org/licenses/by/4.0/>).